Cell and Tissue Research (2019) 378:1–14
https://doi.org/10.1007/s00441-019-03013-x

REGULAR ARTICLE

AAV2/DJ-mediated alpha-synuclein overexpression in the rat substantia nigra as early stage model of Parkinson's disease

Friederike Freiin von Hövel[1,2] · Regina Rumpel[3] · Andreas Ratzka[1] · Dietmar Schreiner[1,2] · Claudia Grothe[1,2]

Received: 22 January 2019 / Accepted: 7 February 2019 / Published online: 15 April 2019

Abstract

Parkinson's disease (PD) is pathologically characterized by the progressive loss of dopaminergic (DA) neurons in the substantia nigra pars compacta (SNpc) and alpha-synucleinopathy. We mimic the disease pathology with overexpression of either the human α-syn wildtype (α-syn-WT) or E46K mutant form (α-syn-E46K) in DA neurons of the SNpc in adult rats using AAV2/DJ as a viral vector for the first time. Transduction efficiency was compared to an equal virus titer expressing the green fluorescent protein (GFP). Motor skills of all animals were evaluated in the cylinder and amphetamine-induced rotation test over a total time period of 12 weeks. Additionally, stereological quantification of DA cells and striatal fiber density measurements were performed every 4 weeks after injection. Rats overexpressing α-syn-WT showed a progressive loss of DA neurons with 40% reduction after 12 weeks accompanied by a greater loss of striatal DA fibers. In contrast, α-syn-E46K led to this reduction after 4 weeks without further progress. Insoluble α-syn positive cytoplasmic inclusions were observed in both groups within DA neurons of the SNpc and VTA. In addition, both α-syn groups developed a characteristic worsening of the rotational behavior over time. However, only the α-syn-WT group reached statistically significant different values in the cylinder test. Summarizing these effects, we established a motor symptom animal model of PD by using AAV2/DJ in the brain for the first time. Thereby, overexpressing of α-syn-E46K mimicked a rather pre-symptomatic stage of the disease, while the α-syn-WT overexpressing animals imitated an early symptomatic stage of PD.

Keywords Parkinson's disease · AAV2/DJ · Alpha-synuclein · Rat model · E46K

Introduction

Parkinson's disease (PD) is a neurodegenerative disorder with variable clinical characteristics as well as different genetic and other underlying neuropathologic mechanisms (Thenganatt and Jankovic 2014). The cardinal motor symptoms resting tremor, rigidity and bradykinesia are directly linked to the decreased level of dopamine within the striatum (ST) due to the loss of dopaminergic (DA) neurons in the substantia nigra pars compacta (SNpc) (Fearnley and Lees 1991). These pathological features are accompanied by the appearance of intracellular protein aggregates called Lewy bodies (LB) and their detection accounts for the definitive diagnosis (Gibb and Lees 1988; Hardy et al. 2006). Lewy bodies mainly consist of the misfolded protein alpha-synuclein (α-syn) and appear in different shapes and subcellular locations (Gibb and Poewe 1986; Spillantini et al. 1997). Normally, the soluble α-syn is abundant in the brain and although its physiological function is still poorly understood, neuropathological changes in PD were shown to correlate with α-syn levels and its aggregation (Azeredo da Silveira et al. 2009; Koprich et al. 2011; Shibayama-Imazu et al. 1993).

While PD is mainly an idiopathic disease, a genetic background can be found in at least 10% of the patients (Gasser 2009). Among these, three missense mutations (A30P, E46K, A53T) in the α-syn-encoding gene (*SNCA*) have been found to cause early onset of PD (Kruger et al. 1998; Polymeropoulos

Friederike Freiin von Hövel and Regina Rumpel contributed equally to this work.

✉ Claudia Grothe
Grothe.Claudia@mh-hannover.de

[1] Institute of Neuroanatomy and Cell Biology, Hannover Medical School, OE 4140, Carl-Neuberg-Str. 1, 30625 Hannover, Germany

[2] Center for Systems Neuroscience (ZSN), Hannover Medical School, Institute of Neuroanatomy and Cell Biology, Carl-Neuberg-Strasse 1, 30625 Hannover, Germany

[3] Institute for Laboratory Animal Science and Central Animal Facility, Hannover Medical School, OE 8600, Carl-Neuberg-Str. 1, 30625 Hannover, Germany

et al. 1997; Zarranz et al. 2004). Additionally, duplication and triplication of the wildtype *SNCA* gene have been associated with autosomal dominant PD (Ibanez et al. 2004; Singleton et al. 2003). To further investigate the development of PD and to establish new therapeutic approaches for the reverse or slowing of disease progression, reliable animal models, which closely mimic the disease phenotype and pathology, are important (Burton et al. 2003).

The fact that elevated levels of α-syn lead to PD pathology has been extensively exploited to generate animal models with greater construct and face validity. One of the widely used models is the adeno-associated virus (AAV)–mediated overexpression of α-syn in DA neurons by stereotactic injection of the viral vectors into the SNpc. The use of AAV vectors offers several advantages including the lack of pathogenicity combined with efficient transduction of different cell types and long-term transgene expression (Wu et al. 2006). The majority of previously published studies used recombinant AAV serotype 2 to transduce mammalian brain cells. However, several other AAV serotypes overexpressing α-syn wildtype (α-syn-WT) or different mutant forms in combination with various promoters and application of variable vector titers were demonstrated to induce a broad range of PD-related behavioral and morphological effects (Albert et al. 2017). Thereby, the cross-packaging of AAV2-derived expression plasmids with capsids from other serotypes (e.g., AAV2/5, AAV2/7, AAV2/8 and AAV2/9) resulted in increased neural tropism and transgene expression (Burger et al. 2004; McFarland et al. 2009; Reimsnider et al. 2007; Van der Perren et al. 2016, 2011). In the last years, several in vitro–engineered AAV capsids have been developed. Among others, AAV2/DJ was created by an adapted DNA family shuffling technology to combine eight different AAV serotypes. Compared to other AAV capsids, this vector was demonstrated to have superior transduction efficiency in vitro (Grimm et al. 2008). Because the transduction efficiency and the level of α-syn expression are crucial parameters for the reliable induction of PD pathology in animal models, we hypothesize that the merging of different wildtype capsids with their unique properties might also be beneficial for the efficient transduction of DA neurons in vivo (Decressac et al. 2012b).

Additionally, the overexpression of certain α-syn mutants has been shown to be superior in their ability to model PD pathology compared to α-syn-WT (Azeredo da Silveira et al. 2009; Lo Bianco et al. 2002; Van der Perren et al. 2015). In this regard, the *SNCA* missene mutation E46K displayed enhanced fibrillization propensity in vitro compared to α-syn-WT and was found to resemble the human LB morphology more closely in a trangsenic mouse model (Emmer et al. 2011; Fredenburg et al. 2007). Besides the transgenic model overexpressing α-syn-E46K, this mutation has only been used in a lentiviral approach so far, where its overexpression led to greater reduction of DA neurons compared to α-syn-A30P and α-syn-WT (Winner et al. 2011).

In this study, we explored the suitability of AAV2/DJ as a vector for an AAV-based rat model of PD for the first time. Furthermore, we compared the effects of α-syn-WT and α-syn-E46K mutant overexpression in DA neurons of the SNpc regarding PD-related morphological and behavioral phenotypes aiming to establish a reliable early motor stage PD animal mode.

Materials and methods

Vector preparation

cDNAs encoding for the green fluorescent protein (GFP), human α-syn-WT, or α-syn-E46K were cloned into the pAAV-MCS plasmid provided with the AAV-DJ helper free expression system (VPK-410-DJ, Cell Biolabs, inc., CA, USA). The CMV promoter in the original pAAV-MCS plasmid was replaced by human synapsin promoter, to ensure neuron-specific expression.

For virus production, 1×10^6 HEK293T cells were seeded onto 15-cm dishes (TPP®, Trasadingen, Switzerland) and transfected on the next day with equimolar amounts of pDJ, pHelper, and pAAV-GFP, pAAV-α-syn-WT, or pAAV-α-syn-E46K plasmids, respectively, using a 3:1 ratio of polyethylenimine (PEI, Sigma-Aldrich, Munich, Germany) according to the published protocol (Huang et al. 2013). Forty-eight to 72 h post-transfection, cells were harvested and viral particles were purified as previously described (Zolotukhin et al. 2002). Briefly, after centrifugation (3,000 × *g*, 5 min), the cell pellet was lysed in 2 ml lysis buffer (50 mM Tris HCl (pH 8.0), 150 mM NaCl) per plate followed by three freeze and thaw cycles. Cell lysates were supplemented with benzoase buffer (500 mM Tris-HCl (pH 8.0), 10 mM MgCl2, 1 mg/ml BSA) mixed with 50 U/ml benzoase (70746, Novagen®, Søborg, Denmark) and incubated for 30 min at 37 °C followed by 30 min centrifugation at 4,000 × *g* to discharge cell debris. The supernatant was transferred onto a discontinuous iodixanol gradient (54%, 40%, 25% and 15%) prepared in Optiseal polypropylene centrifuge tubes (Beckman Coulter, CA, USA) with OptiPrepTM (AXIS-SHIELD PoC AS, Oslo, Norway) and centrifuged for 70 min in a Ti70 rotor at 18 °C with 63,000 × g. Two to 4 ml of the 40% phase containing viral particles were collected with a 21 gauge cannula. The collected fraction was washed three times with phosphate-buffered saline (PBS, Biochrom, Germany) before concentration with Amicon® Ultra-15 centrifugal filters (Merck Millipore, Dublin, Ireland). Aliquots were stored at − 80 °C.

Genome copy viral titers were ascertained via quantitative PCR similar to Huang et al. (2013) using the StepOnePlus Instrument (Applied Biosystems, Darmstadt, Germany). Five microliters of virus solution were incubated with 3 U DNase

(QIAGEN, Hilden, Germany) for 1 hour at room temperature before 2.5 μl of proteinase K (Roche, Mannheim, Germany) was added and incubated 1 h at 65 °C followed by 20 min at 95 °C. For PCR analysis, WPRE forward (5′-TGG CGT GGT GTG CAC TGT-3′) and reverse (5′-CCC GGA AAG GAG CTG ACA-3) primer (Eurofins Genomics, Ebersberg, Germany) were used together with SYBR-Green in tenfold serial dilution. The titer was evaluated compared to a standard curve using pAAV-GFP or pAAV-α-syn plasmids dilution series. A non-template control was also performed.

Purification assay and transduction efficiency in vitro

Ten microliters of the virus solution were incubated with equal amounts of Laemmli buffer at 95 °C for 5 min before separated by sodium dodecyl gel electrophoresis (SDS-page) on a 10% gel according to Zolotukhin et al. (2002). Coomassie brilliant blue staining was performed over night to ensure solutions content and purity grade.

Transduction efficiency of AAV2/DJ preparations carrying GFP, α-syn-WT, or α-syn-E46K was analyzed in vitro on primary cultures of DA progenitor cells. The ventral mesencephalon of embryonic day 12 old rat embryos was dissected and cultivated as previously described (Timmer et al. 2006). Briefly, 80,000 cells were seeded in 24-well NuncTM plates (Thermo Fisher Scientific, Roskilde, Denmark) for 1 day of attachment followed by 2 days of differentiation. For media compositions, see Ratzka et al. (2012). The cells were transfected with 1 μl virus solution in 400 μl differentiating medium for 3 days before changing to virus free medium for additional 4 days. Cells were fixed with 4% paraformaldehyde (PFA, Sigma-Aldrich, Munich, Germany), blocked with PBS containing 0.3% TritonX, 3% normal goat serum (NGS, GibcoTM, Life technologies, Warrington, UK), and 1% bovine serum albumin (BSA, Sigma-Aldrich, Munich, Germany). For immunocytochemistry, cells were incubated overnight with primary anti-TH (AB 152, Millipore, 1:1000) and anti-GFP (1814 460, Roche, 1:200), or anti-α-syn (MS-1572-P1, Thermo Fisher Scientific, 1:1000) antibodies in PBS containing 1% NGS and 0.3% TritonX. Secondary anti-mouse antibodies were conjugated with Alexa488 (a 11034, Invitrogen, 1:500). Secondary anti-rabbit antibodies were conjugated with Alexa555 (A-21429, Invitrogen, 1:500). Transduction efficiency was calculated 3 days after viral vector application with an inverse microscope (IX70, Olympus) using a × 20 magnification by counting of either GPF+, or α-syn+ and TH+ double-labeled cells. Therefore, at least ten randomly selected fields (equivalent to 1% of the area) with a minimum of 150 TH+ cells in total were counted.

Animals and surgical procedure

Seventy-two adult female Sprague Dawley rats from Janvier (France) weighting 225–250 g at the start of the experiments were housed in cages of two to four with food and water available ad libitum. The animals were kept in temperature- and humidity-controlled rooms on a 14-h light/10-h dark schedule. All experimental protocols were permitted by the local authorities (Bezirksregierung LAVES Hannover, Germany) and followed the German Animal Protection Act (33.12-42502-04-15/1993).

All rats received a unilateral stereotactic injection under general chloral hydrate (370 mg/kg; i.p.) anesthesia. Animals were fixed in a stereotactic frame (Stoelting Co., Illinois, USA) and 3 μl virus solution were injected at a rate of 0.3 μl/min above the right substantia nigra using a 10 μl Gastight Hamilton Syringe with a 33 gauge needle (1701 Small Hub RN; Hamilton) (AP − 5.2 mm, LAT − 2.0 mm, and DV − 7.2 mm (values with reference to bregma and dura)) (Paxinos and Watson 2007). After injection, the needle was left in place for an additional 5 min to allow diffusion before slow withdrawal. Dipyrone (200 mg/kg; s.c.) was injected prior to surgery as analgetic treatment, which was continued via drinking water for 3 days post-surgery. At the end of the surgery, animals were provided with 0.9% saline s.c. and were closely monitored until regaining full consciousness.

In a pilot study, the compatibility of the AAV2/DJ in brain tissue was evaluated by stereotactic injection of an empty AAV2/DJ vector into the SNpc of two adult rats (high titer, 2.4×10^9 gc/μl). This was followed by a preliminary experiment evaluating the transduction quality of AAV2/DJ-GFP on DA neurons in vivo. Therefore, 14 rats received two different titers of AAV2/DJ-GFP (either low titer, 4.5×10^6 gc/μl; or medium titer, 4.5×10^7 gc/μl) into the right SNpc. Three animals of each group were sacrificed after 4 weeks. The remaining four animals from both groups were sacrificed after 8 weeks for morphological evaluation.

In the second experiment, 56 adult rats were injected with either AAV2/DJ-GFP (4.5×10^8 gc/μl) ($n = 8$), AAV2/DJ-α-syn-WT (4.0×10^8 gc/μl) ($n = 24$), or AAV2/DJ-α-syn-E46K (4.3×10^8 gc/μl) ($n = 24$). All animals were tested in the amphetamine-induced rotation and in the cylinder test, before as well as 4, 8 and 12 weeks after surgery. A subset of animals was sacrificed for morphological evaluation at each time point after vector injection.

Behavioral analysis

Behavioral testing was performed pre-surgery in addition to 4, 8 and 12 weeks after virus injection.

Amphetamine-induced rotation test: the rats were tested for their rotational bias according to Ungerstedt and Arbuthnott (1970)as described previously. After intraperitoneal injection

of D-Amphetamine sulfate (2.5 mg/kg in saline; Sigma-Aldrich, Munich, Germany), right and left full body turns were monitored over a period of 90 min in an automated rotometer bowl with right body turns, ipsilateral to the virus injection, expressed as positive values.

Cylinder test: spontaneous forelimb asymmetry was measured using the cylinder test (Schallert et al. 2000). Briefly, rats were placed in a transparent cylinder in front of two mirrors and monitored for a maximum period of 5 min. Left and right forepaw touches while exploring the glass wall were counted by a person blinded to the group conditions. The contralateral paw use is expressed as percentage of 20 total wall contacts.

Perfusion and immunohistochemistry

Animals were perfused 4, 8 and 12 weeks post-surgery as described previously (Rumpel et al. 2015). Briefly, deeply anesthetized rats were transcardially perfused with 150 ml 0.9% saline followed by 250 ml of 4% PFA in PBS (Sigma-Aldrich). After post-fixation overnight, the brains were transferred to 30% sucrose (Roth, Karlsruhe, Germany) for cryoprotection. After freezing, brains were coronally sectioned on a freezing stage microtome at 40-μm thickness in series of six.

Immunohistochemical stainings were performed on free-floating sections. The primary antibodies mouse anti-α-syn (610787, BD Biosciences, 1:500), rat anti-DAT (MAB369, Millipore, 1:500), mouse anti-GFP (1814 460, Roche, 1:200) and mouse anti-TH (T1299, Sigma-Aldrich, 1:500) followed by the avidin–biotin complex ABC kit (Vector Laboratories, Peterborough, UK) with biotinylated rabbit anti-mouse antibody (Dako, Glostrup, Denmark, 1:200) or goat anti-rat peroxidase antibody (A 9037, Sigma-Aldrich, 1:100) and DAB (Sigma-Aldrich) with ammonium nickel sulfate intensification were used. Every third section was processed for double immunofluorescence staining with rabbit anti-TH (AB152, Millipore, 1:500) with either mouse anti-GFP (1814 460, Roche, 1:200) or mouse anti-α-syn (610787, BD Biosciences, 1:500). Additional exemplary series were double stained with mouse anti-TH (T1299, Sigma-Aldrich, 1:500) and rabbit anti-phospho α-syn S129 (AB59264, Abcam, 1:2000), rabbit anti-VMAT2 (20042, Immunostar, 1:5000), and mouse anti-α-syn (610787, BD Biosciences, 1:500) or rabbit anti-Iba1 (019-19741, Wako, 1:1000) and mouse anti-GFAP (G3893, Sigma-Aldrich, 1:400). Secondary anti-mouse antibodies were conjugated with Alexa555 (A-21422, Invitrogen, 1:500) or Alexa488 (A32723, Invitrogen, 1:500) and secondary anti-rabbit antibodies with Alexa555 (A-21429, Invitrogen, 1:500) or Alexa488 (A-11034, Invitrogen, 1:500). Nuclei were visualized by 4′,6-Diamidin-2-phenylindol (DAPI) (Sigma-Aldrich, 1:1500) staining.

For proteinase K digestion, single free-floating sections were treated with either 10 μg/ml proteinase K (PK) (03115879001, Roche) in TBS-T (10 mM Tris–HCl, pH 7.8; 100 mM NaCl; 0.1% Tween-100) or TBS-T alone for 30 min at room temperature followed by three washes before treatment with mouse anti-α-syn (610787, BD Biosciences, 1:500) or rabbit anti-phospho α-syn S129 (AB59264, Abcam, 1:2000) and DAB as described above.

All depicted images were taken with an Olympus BX51 or BX60 microscope equipped with a XM-10 camera (Olympus, Hamburg, Germany). Size, contrast and brightness of the images as well as composition of figures and labeling were adjusted using Photoshop CS2 (Adobe Systems Software, Dublin, Ireland).

Cell counting and striatal fiber densitometry

For estimating the total number of DA neurons within the SNpc, every third section was evaluated using the optical fractionator workflow of StereoInvestigator® software (MBF Biosciences, VT, USA) coupled with an Olympus microscope (BX51, Olympus) under × 40 magnification. A minimum of 17 sections per animal including the whole SNpc was counted using a 200 × 200 μm grid size, 110 × 110 μm counting frame and 2 μm guard zone by a user blinded to the experimental conditions. The tissue thickness was determined at each counted section. Results represent estimated population using mean section thickness with counts. A coefficient of error < 0.05 (Gundersen m = 1) was accepted.

Striatal TH+ fiber density was analyzed by densitometry as described previously (Rumpel et al. 2015). Optical density (OD) of the left and right ST was measured on TH-stained brain sections at six coronal levels: AP + 1.6, + 1.2, + 0.8, + 0.4, ± 0.0, − 0.4 mm relative to bregma (Paxinos and Watson 2007) using ImageJ software (National Institutes of Health, Bethesda, MD, USA). The OD of the corpus callosum was set as background and subtracted from the other values. Results are expressed as percentage remaining fibers within the right ST corresponding to the contralateral site.

Statistical analysis

All applied statistics were done using GraphPad Prism software (version 6). All values are presented as mean ± SEM. Comparisons between or within the groups were conducted using a two-way ANOVA followed by post hoc test as indicated. Correlation analysis was performed using linear regression. Statistical significance was set at $p < 0.05$.

Results

Transduction qualities of AAV2/DJ in vitro and in vivo

In a first attempt, we evaluated the efficiency of AAV2/DJ to infect DA neurons by applying GFP carrying AAV2/DJ vector solution to DA rat progenitor cells in vitro. Mean estimated transduction efficiency of (TH+/GFP+) cells was 60.3% (Fig. 1a–c). Additionally, by comparison with non-infected cultures, no reduction of TH expression was observed.

After this, we evaluated the AAV2/DJ compatibility in brain tissue by stereotactic injection of an empty vector into the SNpc ($n = 2$). Staining for TH expression as well as glial fibrillary acidic protein (GFAP) and DAPI after 3 weeks gave no indication of incompatibility of the vector compared to the non-injected hemisphere. Therefore, we evaluated the transduction efficiency of DA neurons in vivo by unilateral stereotactic injection of low and medium titers of the AAV2/DJ carrying GFP into the right SNpc of adult rats (low titer, 4.5×10^6 gc/μl; medium titer, 4.5×10^7 gc/μl). The expression of GFP in DA neurons was examined after 4 ($n = 3$ per group) and 8 weeks ($n = 4$ per group). Transduction efficiency after 4 weeks in vivo was 53.0 ± 8.3% (low titer) and 46.6 ± 8.8% (medium titer). After 8 weeks, the transgene was still expressed in both approaches but to a lower extent, with low titer 35.2 ± 3.2% (Fig. 1d–f) and medium titer 36.9 ± 6.4% (Fig. 1g–i). Both titers did not induce a significant reduction of TH+ cells within the right SNpc compared to the healthy contralateral side (data not shown).

Impact of AAV2/DJ-α-syn-WT and AAV2/DJ-α-syn-E46K overexpression in the rat SN

Expression pattern and distribution of AAV2/DJ-mediated α-syn overexpression

Fifty-six adult rats received a unilateral injection of AAV2/DJ carrying human α-syn-WT, α-syn-E46K mutant, or GFP into the right SNpc (α-syn-WT, 4.0×10^8 gc/μl; α-syn-E46K, 4.3×10^8 gc/μl; GFP, 4.5×10^8 gc/μl). Before in vivo injection, the purity of the vector solution was verified and transduction efficiencies of the vector stocks were evaluated in vitro on DA rat progenitor cells as described to ensure comparability of the α-syn overexpression (α-syn-WT, 43.6%; α-syn-E46K, 44.4%). Morphological and behavioral changes were evaluated 4, 8 and 12 weeks after surgery and compared with healthy values collected before stereotactic injection.

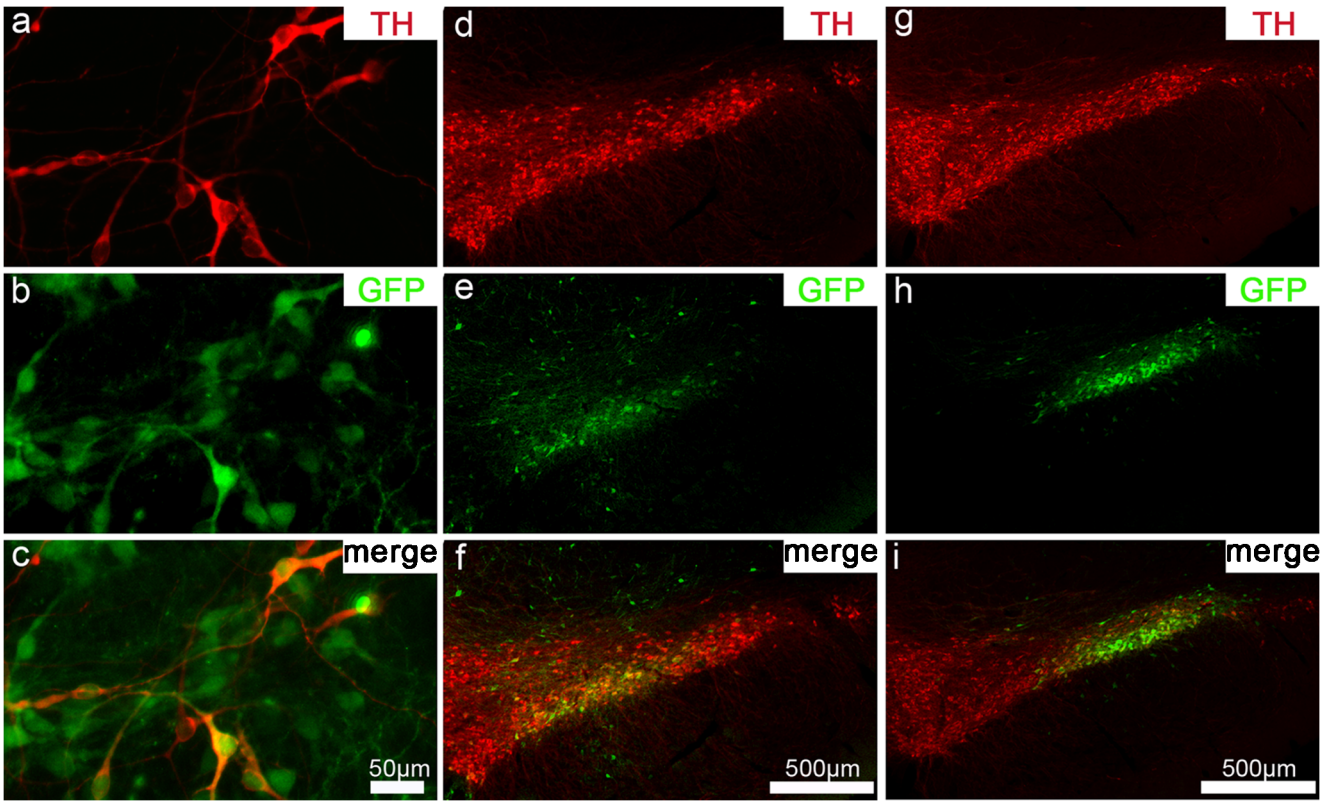

Fig. 1 Transduction qualities of AAV2/DJ carrying GFP in vitro and in vivo. Immunohistochemical staining of DA progenitor cells 3 days after application of AAV2/DJ carrying GFP (a–c). Exemplary midbrain sections of the SNpc 8 weeks after stereotactic injection of low (d–f) or medium vector titer (g–i) demonstrate the transduction of TH+ (red) and GFP+ (green) cells. GFP staining reveals that, especially but not exclusively, DA neurons were transduced in vitro as well as in vivo (b, e, h)

To confirm the expression of α-syn or GFP in SNpc neurons for follow-up morphological analysis, we performed double immunofluorescence staining for TH and human α-syn or GFP, respectively (Fig. 2). Robust expression of all transgenes was observed in DA neurons within the SNpc over the whole experimental time period. A few cells located within the substantia nigra pars reticulata (SNpr) and ventral tegmental area (VTA) as well as other neurons, especially along the needle tract, also displayed transgene expression. Nevertheless, DAB staining confirmed the main localization

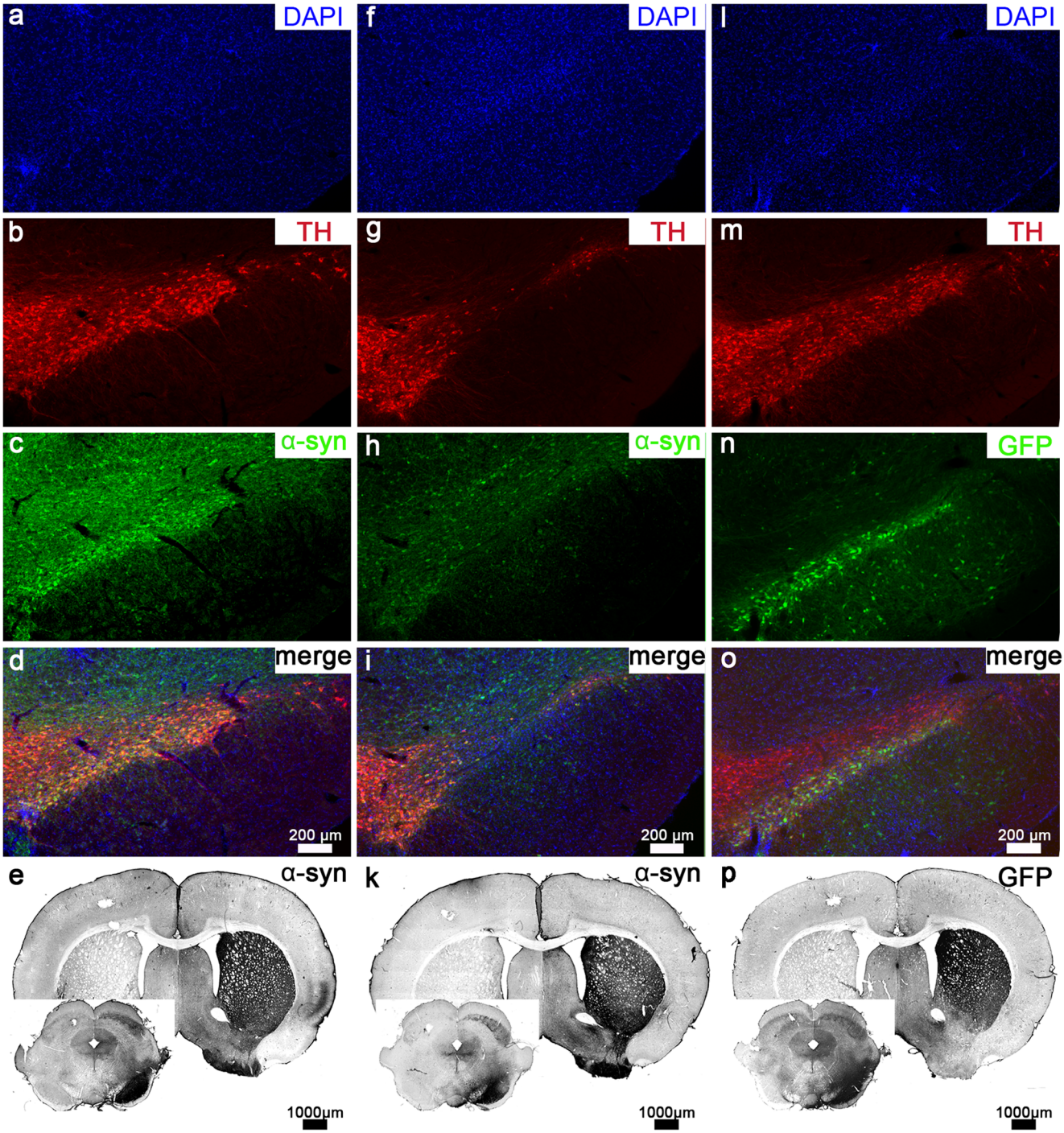

Fig. 2 Transgene expression 4 weeks after unilateral AAV2/DJ injection. Immunohistochemistry of α-syn-WT **(**a–e**)**, α-syn-E46K **(**f–k**)** and GFP **(**l–p**)**–injected animals 4 weeks after surgery. Cell nuclei are stained with DAPI (blue; a, f, l). TH staining (red) shows only minimal reduction of TH+ cells in the a-syn-WT group (b) at this time point, while an obvious reduction was visible in the α-syn-E46K injected group (g) compared to the GFP control animals (m). Staining of α-syn and GFP (green; c, h, n) displays transgene expression in the right SNpc. DAB staining of α-syn-WT (e), α-syn-E46K (k) and GFP (p) demonstrates corresponding transgene expressions in the ST, while the left hemisphere is clear

of transgene expression within the SNpc. The ipsilateral right ST also showed high immunoreactivity of the injected transgene indicating anterograde transport within the axons of the transduced cells (Fig. 2e–p).

Specific staining against the S129-phosphorylated α-syn form (pS129-α-syn), which is known to accumulate preferentially in LBs (Anderson et al. 2006), displayed enhanced phosphorylated α-syn within the injected SNpc compared to the other hemisphere after α-syn overexpression. Additionally, performed proteinase K treatment of histological sections revealed insoluble α-syn accumulations in both α-syn overexpressing groups (Fig. 3a–b, i–k exemplary for the 8-week time point), while, in the GFP control animals, no accumulations were seen (Fig. 3r–s). Both methods showed that overexpression of either α-syn-WT as well as α-syn-E46K led to the appearance of Lewy body–like pathology. Proteinase K pretreatment was also performed before specific pS129-α-syn staining and revealed that at least part of the phosphorylated accumulations were insoluble (Fig. 3c–d, l–m, t–u exemplary for the 8-week time point). Double immunofluorescence staining verified the localization of the pS129-α-syn inclusions within the cytoplasm of remaining DA neurons on the injected

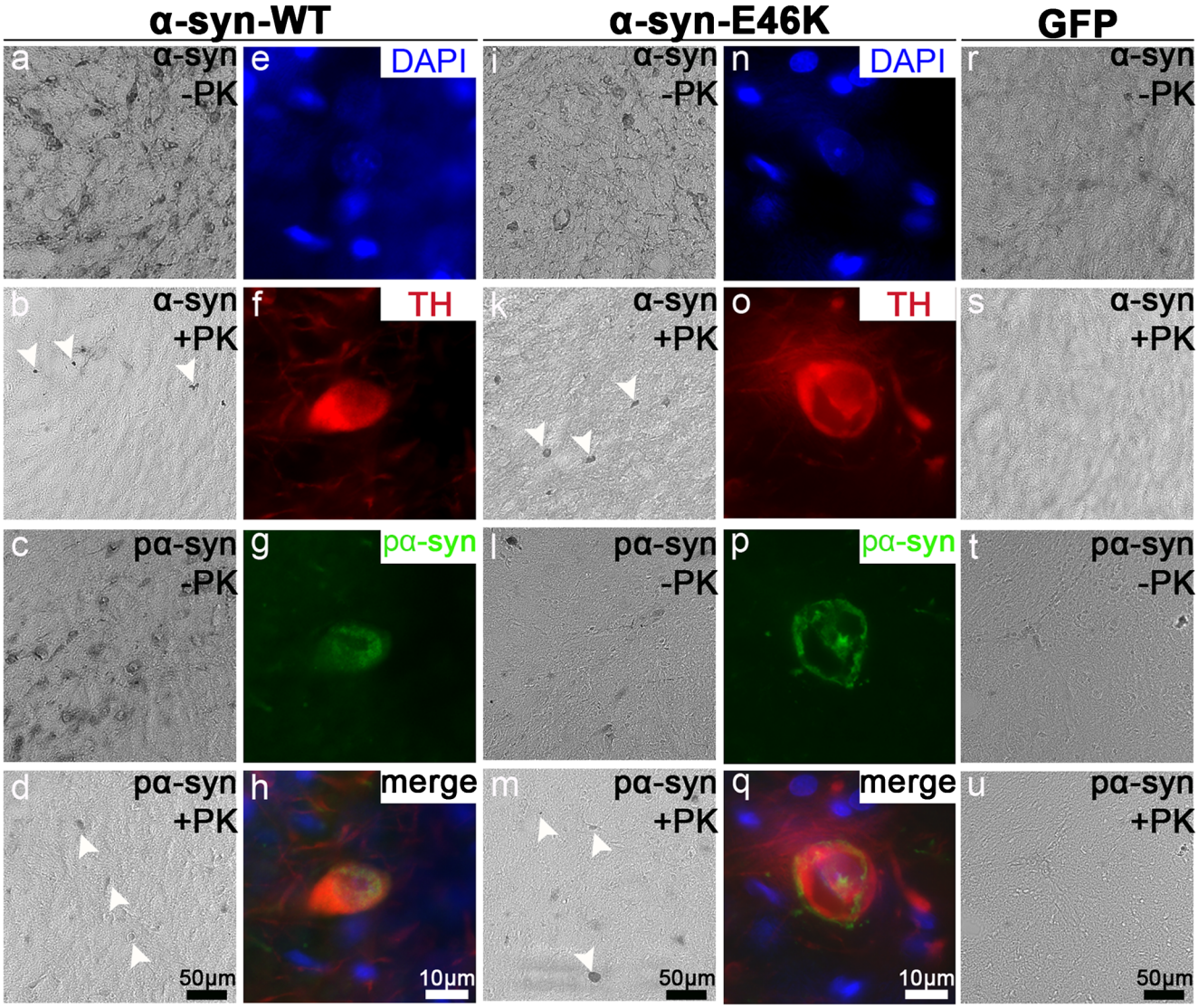

Fig. 3 Animals overexpressing α-syn develop phosphorylated and proteinase K resistant α-syn inclusions within the injected SNpc 8 weeks after viral vector injection. Midbrain sections of animals overexpressing α-syn-WT **(**a–h**)**; α-syn-E46K **(**i–q**)**, or GFP **(**r–u**)** stained against α-syn displayed abroad distribution of overexpressed as well as endogenous α-syn (a, i, r). After proteinase K treatment, only the α-syn overexpressing groups displayed remaining positive accumulations as indicated by white arrow tips (b, k), while none were visible in the GFP control group after 12 weeks (s). Distribution of pS129-α-syn (c, l, t) was more restricted to the SNpc with enhanced appearance in the α-syn-WT group (c). Additional proteinase K pretreatment (d, m, u) revealed similar amounts of resistant inclusions in the α-syn groups as indicated by white arrow tips (d, m). Double immunofluorescence staining showed pS129-α-syn+ cytoplasmatic inclusions (green) within DA neurons (red) of the injected SNpc in both α-syn groups 8 weeks after virus injection (h, q). Cell nuclei were stained with DAPI (blue)

SN (Fig. 3e–h, n–q). Compared to the 4-week time point, pS129-α-syn+ accumulations seemed to increase in both a-syn groups after 8 weeks. After 12 weeks, however, only a few remaining DA neurons of the SNpc were double labeled reflecting the ongoing cell loss (data not shown).

Morphological changes following α-syn-WT and -E46K overexpression in the rat SN

The loss of DA neurons in the injected SNpc and concomitant reduction of DA fiber density within the related ST following α-syn overexpression was quantified 4, 8 and 12 weeks after viral vector injection. Within the injected hemisphere, single animals displayed enhanced cell accumulations, although same vector stocks were used and purity of the solutions was confirmed before injection. This observation, however, was mainly restricted to the needle tract. To determine a possible immunological response, GFAP and Iba1 staining was performed and revealed activation of astrocytes and microglia in exactly these areas (data not shown). Because of the unknown effect of this response on DA neuron loss caused by α-syn overexpression, these animals were excluded from the study. Remaining DA neurons within the injected SNpc were stereologically quantified in all animals included in the study (Fig. 4a, b). The estimated number of DA neurons on the uninjected hemisphere was consistent with earlier reports (Koprich et al. 2010; Nair-Roberts et al. 2008). Animals overexpressing α-syn-WT showed a progressive loss of DA neurons within the injected SNpc during the whole experimental period with 78.3% (± 9.7%) remaining TH+ neurons after 4 weeks, 77.8% (± 7.3%) after 8 weeks and 58.0% (± 3.2%) at the end of the study. In contrast, at the earliest time point, the α-syn-E46K group displayed greater reduction with 62.0% (± 5.3%) remaining TH+ neurons, which did not further decrease over the experimental period (8 weeks, 62.8 ± 7.2%; 12 weeks, 66.7 ± 10.6%; Fig. 4a). Surprisingly, unlike the results of our preliminary test, also the GFP group showed a reduction of TH+ cells on the injected SNpc after 12 weeks (73.1 ± 4.8% remaining TH-labeled cells; Fig. 4b). Nevertheless, while the interference of TH expression due to GFP has already been reported by others (e.g., Febbraro et al. 2013), both α-syn groups displayed significantly greater TH cell loss on the injected SNpc compared to the contralateral hemisphere at the 12-week time point (Fig. 4b). Additional histological sections were stained against vesicular monoamine transporter (VMAT2) to verify that, due to α-syn overexpression, this is downregulated together with TH. The estimated number of remaining VMAT2+ neurons was in line with the TH expression in all groups after 12 weeks as seen in other viral vector studies (α-syn-WT, 6958.3 ± 332.3 TH+ and 6204 ± 716.6 VMAT2+ neurons; α-syn-E46K, 6769.6 ± 665 TH+ and 6343.7 ± 758 VMAT2+ neurons; GFP, 9240.1 ± 631 TH+ and 8483.9 ± 814 VMAT2+ neurons) (Decressac et al. 2012a; Gaugler et al. 2012).

To determine the effect of TH+ cell loss on innervation of the related ST, the density of TH+ fibers was analyzed at six different coronal levels (AP: + 1.6; + 1.2; + 0.8; + 0.4 AP: 0.0; and − 0.4 relative to bregma) (Fig. 4c). Both α-syn overexpressing groups displayed significantly reduced TH+ fiber density in the ipsilateral ST over time (Fig. 4d–e). The α-syn-E46K group showed a prominent 62.0% (± 5.3%) reduction of TH+ fibers at 4 weeks, which did not significantly change over time (8 weeks: 62.7 ± 7.2%; 12 weeks: 66.7 ± 10.7%). On the other hand, in the α-syn-WT overexpressing animals, TH+ fiber loss was more progressive over time. After 4 weeks, TH+ fiber density was reduced to 67.0% (± 5.7%) and decreased further (8 weeks: 58.7 ± 9.4%; 12 weeks: 44.1 ± 6.6%; Fig. 4d). Notably, the striatal fiber density was over 10% lower than the remaining DA neuron number at each time point. Histology of the SN and corresponding ST clearly marked the ongoing degeneration in the α-syn-WT group (Fig. 4f–h) with a strong correlation between the remaining number of DA neurons and TH+ fiber density in the ST over time (α-syn-WT: $R^2 = 0.27$). Additional DAT staining was performed on exemplary selected α-syn-WT injected animals at each time point to confirm striatal fiber loss and revealed similar findings as seen with TH immunoreactivity (data not shown). As seen with DA neuron loss, striatal TH+ fiber density measurements of the GFP group also revealed a reduction after 12 weeks (68.0 ± 5.5% TH+ fibers, Fig. 4e).

Behavioral outcome following α-syn-WT and α-syn-E46K overexpression in the rat SN

To analyze the behavioral alterations triggered by unilateral α-syn overexpression, the motor performance of all animals was evaluated before (− 1) as well as 4, 8 and 12 weeks after viral vector injection. All animals were evaluated in the amphetamine-induced rotation test and the cylinder test.

The GFP control animals did not show any changes in motor behavior over time, neither in the amphetamine-induced rotation test (pre-test: 0.4 ± 1.2; 4 weeks: 0.0 ± 1.5; 8 weeks: 0.4 ± 1.5; 12 weeks: − 0.3 ± 1.6 full body turns per minute; Fig. 5a), nor in the cylinder test (pre-test: 47.5 ± 1.0%; 4 weeks: 43.8 ± 3.4%; 8 weeks: 47.5 ± 3.0%; 12 weeks: 43.8 ± 4.1% left paw usage; Fig. 5b). The α-syn-WT overexpressing rats showed substantially increasing contralateral rotational behavior over time (pre-test: − 0.2 ± 0.8; 4 weeks: − 1.4 ± 1.0; 8 weeks: − 2.6 ± 1.1; 12 weeks: − 3.7 ± 1.9 full body turns per minute), although this did not reach significance (Fig. 5a). However, α-syn-E46K overexpressing animals developed significant ipsilateral rotational behavior over time (pre-test: 0.0 ± 0.7; 4 weeks: − 0.7 ± 1.0; 8 weeks: 0.9 ± 1.4; 12 weeks: 2.6 ± 2.5 full body turns per minute; Fig. 5a). With regard to

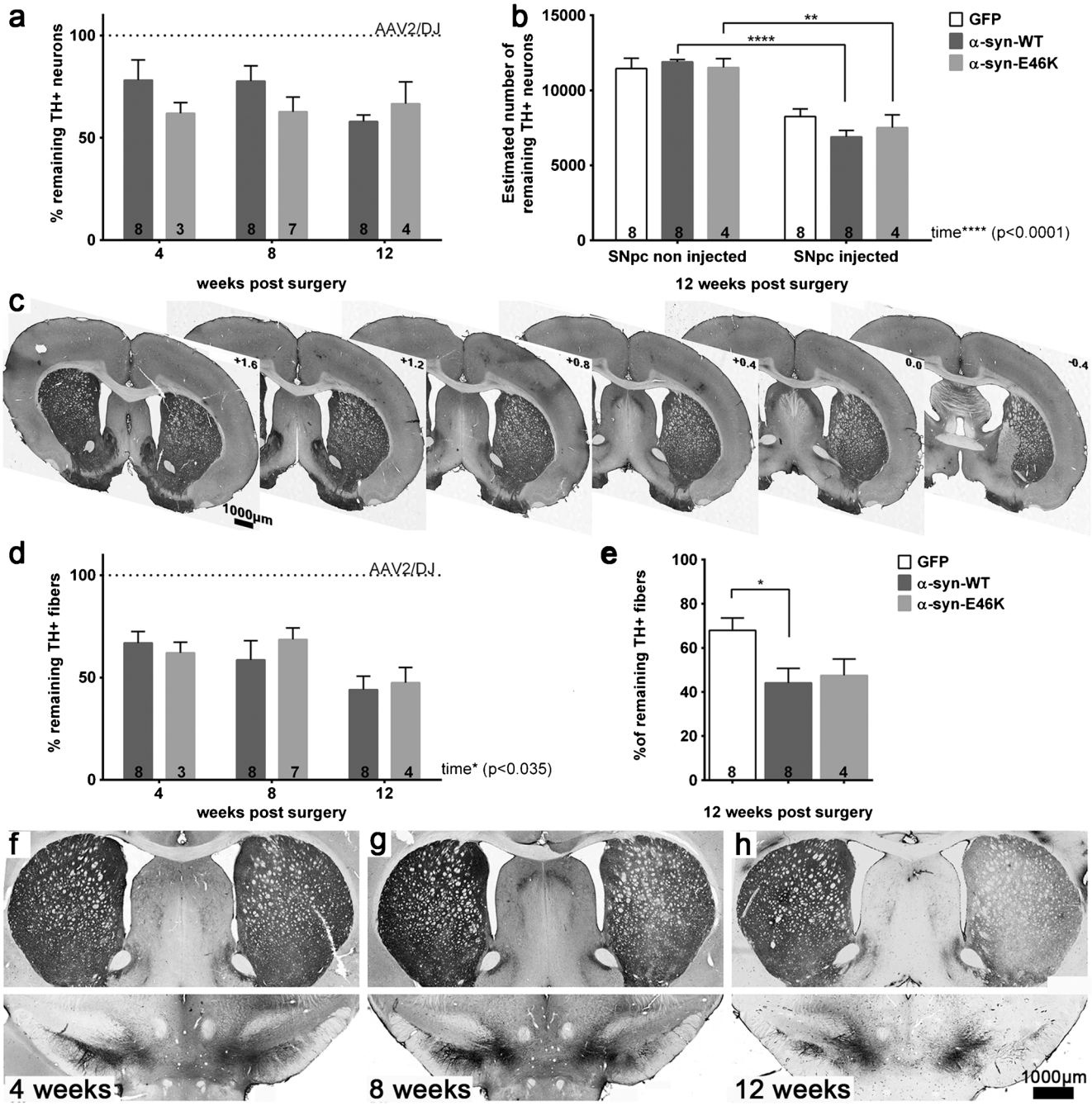

Fig. 4 Quantification of the histomorphological changes following α-syn overexpression in the SNpc. Percentage of remaining TH+ neurons in the injected SNpc of animals overexpressing α-syn over the whole experimental period in comparison to the results of animals injected with the AAV2/DJ empty vector (dotted line) verified loss of DA neurons already after four weeks (a). The estimated number of TH+ cells within the injected SNpc as well as the contralateral hemisphere of all groups at 12 weeks revealed significant differences in both α-syn groups (b). For TH+ fiber density measurements, serial sections of six different rostro-caudal striatal planes relative to bregma according to Paxinos and Watson (2007) were analyzed (c). Percentage of remaining TH+ fibers in the ipsilateral ST of animals overexpressing α-syn over the whole experimental period in comparison to animals injected with the AAV2/DJ empty vector (dotted line) confirmed the stereological results (d). The percentage of remaining TH+ fibers in the ipsilateral ST of all groups at the end of the study showed significant differences between GFP control animals and animals overexpressing α-syn-WT (e). The progression of degeneration in the SNpc and corresponding ST is visualized on exemplary TH DAB–stained sections of animals overexpressing α-syn-WT at all experimental time points post-surgery (f–h). Data are presented as mean ± SEM and number of animals analyzed as indicated in each graph. Two-way ANOVA followed by Bonferroni's post hoc analysis (a, d) or by Sidak's post hoc analysis (b, e) with $*p < 0.05$, $**p < 0.005$, $****p < 0.0001$ as indicated in each panel

the cylinder test, the α-syn-E46K group did not develop an obvious reduction in left forepaw usage and reached similar values as the GFP control animals (pre-test: 49.3 ± 1.4%; 4 weeks: 45.0 ± 2.3%; 8 weeks: 49.6 ± 2.4%; 12 weeks:

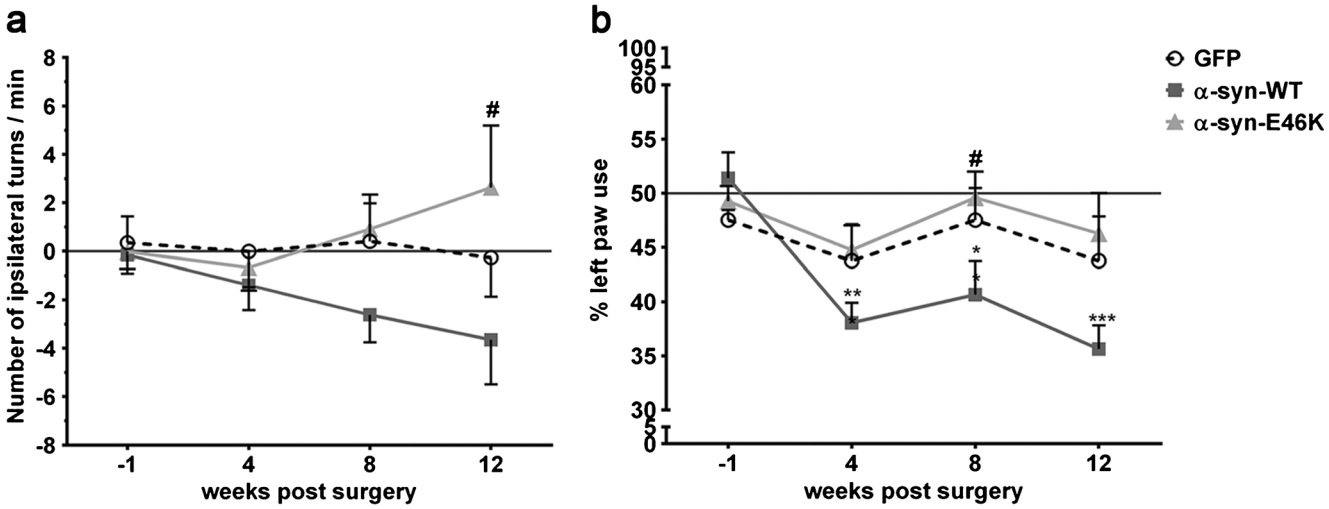

Fig. 5 Behavioral outcome in the amphetamine-induced rotation and cylinder tests before as well as 4, 8 and 12 weeks after viral vector injection. Number of full body turns after single amphetamine injection were counted over 90 min with ipsilateral turns expressed as positive values for all animals at every time point post-surgery (a). Left forepaw usage in the cylinder test is given as percentage of total wall touches for all animals over the whole experimental time period (b). Data are presented as mean ± SEM. Two-way ANOVA followed by Tukey's post hoc analysis with $^{**}p < 0.05$ and $^{***}p < 0.001$ compared to pre-test values within the same group and $^{\#}p < 0.05$ compared between α-syn-WT and α-syn E46K at the same time point. (n for α-syn-WT: pre-test/four 4 weeks: 18; 8 weeks: 15; 12 weeks: 8; α-syn-E46K: pre-test/4 weeks: 20; 8 weeks: 12; 12 weeks: 4; GFP: at every time point: 8)

46.3 ± 3.8% left paw usage; Fig. 5b). In opposition, rats overexpressing α-syn-WT revealed a significant reduction of left forepaw usage at every time point post-surgery compared to the evaluated baseline values in the pre-test (pre-test: 51.4 ± 2.4%; 4 weeks: 38.1 ± 1.9%; 8 weeks: 40.7 ± 3.1%; 12 weeks: 35.6 ± 2.2% left paw usage) (Fig. 5b).

Discussion

The aim of this study was to generate a reliable animal model of an early stage of PD with high motor face validity. Therefore, we compared the morphological and behavioral outcomes following α-syn-WT and α-syn-E46K overexpression regarding PD related phenotypes over 12 weeks. Before this, we evaluated the compatibility of AAV2/DJ as viral vector in brain tissue for the first time hypothesizing that this vector occupied enhanced transduction efficiency of DA neurons.

Our morphological findings suggest that AAV2/DJ is highly efficient to transduce DA neurons with long-lasting transgene expression for up to 12 weeks. The compatibility of the AAV2/DJ in brain tissue was confirmed by injection of an empty vector without visible microglia activation or loss of DA neurons.

Overexpressing of either α-syn-WT or α-syn-E46K resulted in an evident neuronal loss combined with enhanced formation of phosphorylated α-syn aggregations within the injected SNpc. Although these α-syn accumulations do not exclusively appear in PD patients, their appearance defines the diagnosis (Cookson and van der Brug 2008; Goedert et al. 1998). However, it remains unclear, whether α-syn aggregation represents a physiological or pathological reaction of the neuron. Double immunofluorescence staining verified their localization in the cytoplasm of remaining DA neurons in the injected SNpc as well as in neurons of the VTA at every time point post-surgery. Additionally, we could show that part of these inclusions were resistant towards proteinase K treatment. Therefore, we recapitulate that overexpression of α-syn-WT as well as α-syn-E46K in the rat SNpc results in highly phosphorylated and insoluble α-syn inclusions mimicking human LB like pathology.

Also, overexpression of α-syn-WT as well as α-syn-E46K resulted in irreversible morphological changes in the dopaminergic nigrostriatal pathway. While animals of the α-syn-WT group displayed an ongoing progressive loss of TH expression in the SNpc as well as in the ipsilateral ST, α-syn-E46K seemed to be more toxic leading to similar neuronal loss in less time, which did not progress further. However, the results after α-syn-WT overexpression led to the implication that a greater loss of DA neurons could be achievable over a longer time period.

The histomorphological changes following AAV2/DJ-α-syn-E46K injection in this study are comparable to a lentiviral vector approach using the same α-syn mutant (Winner et al. 2011). Compared to both other known point mutations of the *SNCA* gene, which have been transduced with other AAVs in studies with comparable vector titers, overexpression of α-syn-E46K seems to be more toxic than the α-syn-A30P and less toxic than the α-syn-A53T in DA neurons (Gaugler et al. 2012; Koprich et al. 2011; Van der Perren et al. 2015). This observation might be the consequence of the different amyloid

fibrillation forming capacities of the mutations closer characterized in vitro (Winner et al. 2011).

The variety between the so far published viral vector–based α-syn overexpression rat PD models regarding rodent strain, serotype, promoter and working titers as well as the great variability in the model outcomes make it difficult to compare our results (Albert et al. 2018; Dehay and Fernagut 2016). Analysis of studies using AAV serotypes that are incorporated in the AAV2/DJ suggests that the combination of these serotypes did not further enhance the transduction efficiency in DA neurons (Gombash et al. 2013; Gorbatyuk et al. 2008; Kirik et al. 2002; Korecka et al. 2011; McFarland et al. 2009; Van der Perren et al. 2011; Yamada et al. 2004).

Interestingly, we also observed a reduction of TH labeling following GFP expression after 12 weeks. However, this decrease in DA neurons was not significant compared to the contralateral hemisphere and animals did not develop motor impairments. Notably, we did not expect this after excluding viral vector toxicity in vivo prior to the main experiment by evaluating an empty vector with higher titers as well as lower titers of AAV2/DJ carrying GFP, which did not induce histomorphological changes. Nevertheless, also, others reported titer-dependent neuronal loss after transducing DA neurons with GFP by using other AAVs and we propose that a transgene carrying vector is a more appropriate control than an empty vector for these animal models (Klein et al. 2006; Koprich et al. 2011). We point out that the pronounced vulnerability of DA neurons towards transgene overload is a major obstacle in establishing an adequate control (Albert et al. 2017).

The amphetamine-induced rotation and cylinder tests have been widely used to evaluate behavioral changes following α-syn overexpression (Decressac et al. 2012a; Febbraro et al. 2013; Gaugler et al. 2012; Gombash et al. 2013; Kirik et al. 2002). Besides the cell-specific interaction of different α-syn expressions, significant impairments could be expected in the cylinder test (< 35%) and amphetamine-induced rotation test (> 3 turns/min) when at least 45% of TH+ cells and corresponding striatal fibers are lost (Decressac et al. 2012b). In our study, both α-syn overexpressing groups developed increased rotational behavior over time, whereas only animals of the α-syn-WT group displayed significantly reduced forepaw usage in the cylinder test already after 4 weeks, which further decreased, while the α-syn-E46K group had normal behavior. However, even with declines around 40% of DA neurons, the animals were still below the postulated threshold and most probably in a disease stage covered by compensation mechanisms. Indeed, it has been shown earlier that extracellular dopamine content is normalized at disease beginning, which could overshadow motor symptoms (Bergstrom and Garris 2003).

Under drug intervention, these animals displayed dopamine imbalances leading to increased rotations towards the affected hemisphere but without significance due to ranges below the established threshold. In contrast, animals overexpressing α-syn-WT seemed to have overcome the critical limit. Especially the reduced fiber density (increase of more than 50% after 12 weeks) strongly correlates with the deficits displayed in the cylinder test. Correspondingly, they also showed increasing rotational behavior but, unexpectedly, towards the contralateral side. This contradictory contralateral rotational behavior has already been observed previously after α-syn-WT overexpression and could be a consequence of compensation mechanisms as well (Febbraro et al. 2013; Gorbatyuk et al. 2010; Ulusoy et al. 2010). Compensatory mechanisms include increased dopamine synthesis, release and diffusion, which could result in higher dopamine levels after drug intervention, although the hemisphere is more affected (Zigmond et al. 1990). Additionally, other studies showed compensatory sprouting of surviving neurons after progressive neuronal loss within 16 weeks, even though impaired DAT function, dysregulation of dopamine release and diminished dopamine uptake capacity have been reported (Finkelstein et al. 2000; Lee et al. 2008; Stanic et al. 2003).

Next to the possible compensation mechanisms due to dopamine reduction, the effect of α-syn itself has to be taken into account. In vitro analyses showed that α-syn-WT as well as α-syn-A30P decreased dopamine uptake by interacting with DAT, while α-syn-A53T was unable to modulate DAT function (Wersinger et al. 2003). It was shown that α-syn-A53T influences dopamine storage and release via VMAT2 resulting in enhanced dopamine release after amphetamine treatment (Lotharius et al. 2002). It was also postulated that phosphorylated α-syn affects the nigrostriatal terminals, which leads to abnormal dopamine release. Additional in vitro analysis showed similar cellular membrane binding capacities for α-syn-WT and α-syn-E46K as well as morphological analogies, whereas the mutant form displayed enhanced fibrillization activity (Fredenburg et al. 2007). Finally, it was suggested that in early stages of the α-syn rat model, visible motor impairments are a consequence of neuronal dysfunction and in later stages, the combination of neuronal loss combined with dysfunction of the remaining neurons (Decressac et al. 2012a).

Summarizing these effects, we would like to highlight that, in the α-syn PD rat model, the animals suffer from progressive neuron loss at the narrow borderline to the healthy state due to compensatory mechanisms, while impairment only takes place with increasing neuronal cell death. In our case, the α-syn-E46K-overexpressing animals mimicked a presymptomatic stage of PD, where histomorphological changes were masked by compensation mechanisms in their normal activity until uncovered by drug intervention. In contrast, the α-syn-WT overexpressing animals imitated an early symptomatic motor stage of PD, with behavioral impairments

obviously detectable without drug interference. To diagnose such early disease stages with regard to motor deficits, new or more sensitive behavioral tests without drug intervention have to be added. Additionally, treatment with L-DOPA before the behavioral testing will further increase the predictive validity of the model.

Conclusion

In conclusion, we established a suitable animal model of PD based on local overexpression of human α-syn-WT using the viral vector AAV2/DJ. This model has reliable construct and face validity displaying three essential pathological characteristics: α-syn positive cytoplasmic inclusions, gradual degeneration of DA neurons and progressively developing behavioral changes. Imitating an early symptomatic motor stage of PD, this model possesses enhanced predictive validity to evaluate new therapeutic approaches to reverse or slow down the disease progression.

Acknowledgements We thank Hella Brinkmann, Silke Fischer, Natascha Heidrich, Kerstin Kuhlemann and Maike Wesemann (Institute of Neuroanatomy and Cell Biology) for excellent technical assistance.

Funding information This work was financially supported by the Konrad-Adenauer-Stiftung (Friederike Freiin von Hövel).

Compliance with ethical standards

Conflict of interest The authors declare that they have no conflict of interest.

Ethical approval All procedures performed in studies involving animals were in accordance with the ethical standards of the German Animal Protection Act (33.12-42502-04-15/1993). This article does not contain any studies with human participants performed by any of the authors.

Informed consent Not applicable.

References

Albert K, Voutilainen MH, Domanskyi A, Airavaara M (2017) AAV vector-mediated gene delivery to substantia nigra dopamine neurons: implications for gene therapy and disease models. Genes (Basel):8

Albert K, Voutilainen MH, Domanskyi A, Piepponen TP, Ahola S, Tuominen RK, Richie C, Harvey BK, Airavaara M (2018) Downregulation of tyrosine hydroxylase phenotype after AAV injection above substantia nigra: caution in experimental models of Parkinson's disease. J Neurosci Res

Anderson JP, Walker DE, Goldstein JM, de Laat R, Banducci K, Caccavello RJ, Barbour R, Huang J, Kling K, Lee M, Diep L, Keim PS, Shen X, Chataway T, Schlossmacher MG, Seubert P, Schenk D, Sinha S, Gai WP, Chilcote TJ (2006) Phosphorylation of Ser-129 is the dominant pathological modification of alpha-synuclein in familial and sporadic Lewy body disease. J Biol Chem 281:29739–29752

Azeredo da Silveira S, Schneider BL, Cifuentes-Diaz C, Sage D, Abbas-Terki T, Iwatsubo T, Unser M, Aebischer P (2009) Phosphorylation does not prompt, nor prevent, the formation of alpha-synuclein toxic species in a rat model of Parkinson's disease. Hum Mol Genet 18: 872–887

Bergstrom BP, Garris PA (2003) "Passive stabilization" of striatal extracellular dopamine across the lesion spectrum encompassing the presymptomatic phase of Parkinson's disease: a voltammetric study in the 6-OHDA-lesioned rat. J Neurochem 87:1224–1236

Burger C, Gorbatyuk OS, Velardo MJ, Peden CS, Williams P, Zolotukhin S, Reier PJ, Mandel RJ, Muzyczka N (2004) Recombinant AAV viral vectors pseudotyped with viral capsids from serotypes 1, 2, and 5 display differential efficiency and cell tropism after delivery to different regions of the central nervous system. Mol Ther 10:302–317

Burton EA, Glorioso JC, Fink DJ (2003) Gene therapy progress and prospects: Parkinson's disease. Gene Ther 10:1721–1727

Cookson MR, van der Brug M (2008) Cell systems and the toxic mechanism(s) of alpha-synuclein. Exp Neurol 209:5–11

Decressac M, Mattsson B, Bjorklund A (2012a) Comparison of the behavioural and histological characteristics of the 6-OHDA and alpha-synuclein rat models of Parkinson's disease. Exp Neurol 235:306–315

Decressac M, Mattsson B, Lundblad M, Weikop P, Bjorklund A (2012b) Progressive neurodegenerative and behavioural changes induced by AAV-mediated overexpression of alpha-synuclein in midbrain dopamine neurons. Neurobiol Dis 45:939–953

Dehay B, Fernagut PO (2016) Alpha-synuclein-based models of Parkinson's disease. Rev Neurol (Paris) 172:371–378

Emmer KL, Waxman EA, Covy JP, Giasson BI (2011) E46K human alpha-synuclein transgenic mice develop Lewy-like and tau pathology associated with age-dependent, detrimental motor impairment. J Biol Chem 286:35104–35118

Fearnley JM, Lees AJ (1991) Ageing and Parkinson's disease: substantia nigra regional selectivity. Brain 114(Pt 5):2283–2301

Febbraro F, Sahin G, Farran A, Soares S, Jensen PH, Kirik D, Romero-Ramos M (2013) Ser129D mutant alpha-synuclein induces earlier motor dysfunction while S129A results in distinctive pathology in a rat model of Parkinson's disease. Neurobiol Dis 56:47–58

Finkelstein DI, Stanic D, Parish CL, Tomas D, Dickson K, Horne MK (2000) Axonal sprouting following lesions of the rat substantia nigra. Neuroscience 97:99–112

Fredenburg RA, Rospigliosi C, Meray RK, Kessler JC, Lashuel HA, Eliezer D, Lansbury PT Jr (2007) The impact of the E46K mutation on the properties of alpha-synuclein in its monomeric and oligomeric states. Biochemistry 46:7107–7118

Gasser T (2009) Molecular pathogenesis of Parkinson disease: insights from genetic studies. Expert Rev Mol Med 11:e22

Gaugler MN, Genc O, Bobela W, Mohanna S, Ardah MT, El-Agnaf OM, Cantoni M, Bensadoun JC, Schneggenburger R, Knott GW, Aebischer P, Schneider BL (2012) Nigrostriatal overabundance of alpha-synuclein leads to decreased vesicle density and deficits in dopamine release that correlate with reduced motor activity. Acta Neuropathol 123:653–669

Gibb WR, Lees AJ (1988) The relevance of the Lewy body to the pathogenesis of idiopathic Parkinson's disease. J Neurol Neurosurg Psychiatry 51:745–752

Gibb WR, Poewe WH (1986) The centenary of Friederich H. Lewy 1885-1950. Neuropathol Appl Neurobiol 12:217–222

Goedert M, Spillantini MG, Davies SW (1998) Filamentous nerve cell inclusions in neurodegenerative diseases. Curr Opin Neurobiol 8: 619–632

Gombash SE, Manfredsson FP, Kemp CJ, Kuhn NC, Fleming SM, Egan AE, Grant LM, Ciucci MR, MacKeigan JP, Sortwell CE (2013) Morphological and behavioral impact of AAV2/5-mediated

overexpression of human wildtype alpha-synuclein in the rat nigrostriatal system. PLoS One 8:e81426

Gorbatyuk OS, Li S, Sullivan LF, Chen W, Kondrikova G, Manfredsson FP, Mandel RJ, Muzyczka N (2008) The phosphorylation state of Ser-129 in human alpha-synuclein determines neurodegeneration in a rat model of Parkinson disease. Proc Natl Acad Sci U S A 105: 763–768

Gorbatyuk OS, Li S, Nguyen FN, Manfredsson FP, Kondrikova G, Sullivan LF, Meyers C, Chen W, Mandel RJ, Muzyczka N (2010) Alpha-synuclein expression in rat substantia nigra suppresses phospholipase D2 toxicity and nigral neurodegeneration. Mol Ther 18: 1758–1768

Grimm D, Lee JS, Wang L, Desai T, Akache B, Storm TA, Kay MA (2008) In vitro and in vivo gene therapy vector evolution via multispecies interbreeding and retargeting of adeno-associated viruses. J Virol 82:5887–5911

Hardy J, Cai H, Cookson MR, Gwinn-Hardy K, Singleton A (2006) Genetics of Parkinson's disease and parkinsonism. Ann Neurol 60: 389–398

Huang X, Hartley AV, Yin Y, Herskowitz JH, Lah JJ, Ressler KJ (2013) AAV2 production with optimized N/P ratio and PEI-mediated transfection results in low toxicity and high titer for in vitro and in vivo applications. J Virol Methods 193:270–277

Ibanez P, Bonnet AM, Debarges B, Lohmann E, Tison F, Pollak P, Agid Y, Durr A, Brice A (2004) Causal relation between alpha-synuclein gene duplication and familial Parkinson's disease. Lancet 364: 1169–1171

Kirik D, Rosenblad C, Burger C, Lundberg C, Johansen TE, Muzyczka N, Mandel RJ, Bjorklund A (2002) Parkinson-like neurodegeneration induced by targeted overexpression of alpha-synuclein in the nigrostriatal system. J Neurosci 22:2780–2791

Klein RL, Dayton RD, Leidenheimer NJ, Jansen K, Golde TE, Zweig RM (2006) Efficient neuronal gene transfer with AAV8 leads to neurotoxic levels of tau or green fluorescent proteins. Mol Ther 13:517–527

Koprich JB, Johnston TH, Reyes MG, Sun X, Brotchie JM (2010) Expression of human A53T alpha-synuclein in the rat substantia nigra using a novel AAV1/2 vector produces a rapidly evolving pathology with protein aggregation, dystrophic neurite architecture and nigrostriatal degeneration with potential to model the pathology of Parkinson's disease. Mol Neurodegener 5:43

Koprich JB, Johnston TH, Huot P, Reyes MG, Espinosa M, Brotchie JM (2011) Progressive neurodegeneration or endogenous compensation in an animal model of Parkinson's disease produced by decreasing doses of alpha-synuclein. PLoS One 6:e17698

Korecka J, Schouten M, Eggers R, Ulusoy A, Bossers K, Verhaagen J (2011) Comparison of AAV serotypes for gene delivery to dopaminergic neurons in the substantia nigra. Viral Gene Therapy 21. https://doi.org/10.5772/18939

Kruger R, Kuhn W, Muller T, Woitalla D, Graeber M, Kosel S, Przuntek H, Epplen JT, Schols L, Riess O (1998) Ala30Pro mutation in the gene encoding alpha-synuclein in Parkinson's disease. Nat Genet 18:106–108

Lee J, Zhu WM, Stanic D, Finkelstein DI, Horne MH, Henderson J, Lawrence AJ, O'Connor L, Tomas D, Drago J, Horne MK (2008) Sprouting of dopamine terminals and altered dopamine release and uptake in Parkinsonian dyskinaesia. Brain 131:1574–1587

Lo Bianco C, Ridet JL, Schneider BL, Deglon N, Aebischer P (2002) Alpha -synucleinopathy and selective dopaminergic neuron loss in a rat lentiviral-based model of Parkinson's disease. Proc Natl Acad Sci U S A 99:10813–10818

Lotharius J, Barg S, Wiekop P, Lundberg C, Raymon HK, Brundin P (2002) Effect of mutant alpha-synuclein on dopamine homeostasis in a new human mesencephalic cell line. J Biol Chem 277:38884–38894

McFarland NR, Lee JS, Hyman BT, McLean PJ (2009) Comparison of transduction efficiency of recombinant AAV serotypes 1, 2, 5, and 8 in the rat nigrostriatal system. J Neurochem 109:838–845

Nair-Roberts RG, Chatelain-Badie SD, Benson E, White-Cooper H, Bolam JP, Ungless MA (2008) Stereological estimates of dopaminergic, GABAergic and glutamatergic neurons in the ventral tegmental area, substantia nigra and retrorubral field in the rat. Neuroscience 152:1024–1031

Paxinos G, Watson C (2007) The rat brain in stereotaxic coordinates. Elsevier Inc., London

Polymeropoulos MH, Lavedan C, Leroy E, Ide SE, Dehejia A, Dutra A, Pike B, Root H, Rubenstein J, Boyer R, Stenroos ES, Chandrasekharappa S, Athanassiadou A, Papapetropoulos T, Johnson WG, Lazzarini AM, Duvoisin RC, Di Iorio G, Golbe LI, Nussbaum RL (1997) Mutation in the alpha-synuclein gene identified in families with Parkinson's disease. Science 276:2045–2047

Ratzka A, Kalve I, Ozer M, Nobre A, Wesemann M, Jungnickel J, Koster-Patzlaff C, Baron O, Grothe C (2012) The colayer method as an efficient way to genetically modify mesencephalic progenitor cells transplanted into 6-OHDA rat model of Parkinson's disease. Cell Transplant 21:749–762

Reimsnider S, Manfredsson FP, Muzyczka N, Mandel RJ (2007) Time course of transgene expression after intrastriatal pseudotyped rAAV2/1, rAAV2/2, rAAV2/5, and rAAV2/8 transduction in the rat. Mol Ther 15:1504–1511

Rumpel R, Hohmann M, Klein A, Wesemann M, Baumgartner W, Ratzka A, Grothe C (2015) Transplantation of fetal ventral mesencephalic progenitor cells overexpressing high molecular weight fibroblast growth factor 2 isoforms in 6-hydroxydopamine lesioned rats. Neuroscience 286:293–307

Schallert T, Fleming SM, Leasure JL, Tillerson JL, Bland ST (2000) CNS plasticity and assessment of forelimb sensorimotor outcome in unilateral rat models of stroke, cortical ablation, parkinsonism and spinal cord injury. Neuropharmacology 39:777–787

Shibayama-Imazu T, Okahashi I, Omata K, Nakajo S, Ochiai H, Nakai Y, Hama T, Nakamura Y, Nakaya K (1993) Cell and tissue distribution and developmental change of neuron specific 14 kDa protein (phosphoneuroprotein 14). Brain Res 622:17–25

Singleton AB, Farrer M, Johnson J, Singleton A, Hague S, Kachergus J, Hulihan M, Peuralinna T, Dutra A, Nussbaum R, Lincoln S, Crawley A, Hanson M, Maraganore D, Adler C, Cookson MR, Muenter M, Baptista M, Miller D, Blancato J, Hardy J, Gwinn-Hardy K (2003) Alpha-synuclein locus triplication causes Parkinson's disease. Science 302:841

Spillantini MG, Schmidt ML, Lee VM, Trojanowski JQ, Jakes R, Goedert M (1997) Alpha-synuclein in Lewy bodies. Nature 388: 839–840

Stanic D, Finkelstein DI, Bourke DW, Drago J, Horne MK (2003) Timecourse of striatal re-innervation following lesions of dopaminergic SNpc neurons of the rat. Eur J Neurosci 18:1175–1188

Thenganatt MA, Jankovic J (2014) Parkinson disease subtypes. JAMA Neurol 71:499–504

Timmer M, Grosskreutz J, Schlesinger F, Krampfl K, Wesemann M, Just L, Bufler J, Grothe C (2006) Dopaminergic properties and function after grafting of attached neural precursor cultures. Neurobiol Dis 21:587–606

Ulusoy A, Febbraro F, Jensen PH, Kirik D, Romero-Ramos M (2010) Co-expression of C-terminal truncated alpha-synuclein enhances full-length alpha-synuclein-induced pathology. Eur J Neurosci 32:409–422

Ungerstedt U, Arbuthnott GW (1970) Quantitative recording of rotational behavior in rats after 6-hydroxy-dopamine lesions of the nigrostriatal dopamine system. Brain Res 24:485–493

Van der Perren A, Toelen J, Carlon M, Van den Haute C, Coun F, Heeman B, Reumers V, Vandenberghe LH, Wilson JM, Debyser Z, Baekelandt V (2011) Efficient and stable transduction of

dopaminergic neurons in rat substantia nigra by rAAV 2/1, 2/2, 2/5, 2/6.2, 2/7, 2/8 and 2/9. Gene Ther 18:517–527

Van der Perren A, Toelen J, Casteels C, Macchi F, Van Rompuy AS, Sarre S, Casadei N, Nuber S, Himmelreich U, Osorio Garcia MI, Michotte Y, D'Hooge R, Bormans G, Van Laere K, Gijsbers R, Van den Haute C, Debyser Z, Baekelandt V (2015) Longitudinal follow-up and characterization of a robust rat model for Parkinson's disease based on overexpression of alpha-synuclein with adeno-associated viral vectors. Neurobiol Aging 36:1543–1558

Van der Perren A, Casteels C, Van Laere K, Gijsbers R, Van den Haute C, Baekelandt V (2016) Development of an alpha-synuclein based rat model for Parkinson's disease via stereotactic injection of a recombinant adeno-associated viral vector. J Vis Exp:53670

Wersinger C, Prou D, Vernier P, Niznik HB, Sidhu A (2003) Mutations in the lipid-binding domain of alpha-synuclein confer overlapping, yet distinct, functional properties in the regulation of dopamine transporter activity. Mol Cell Neurosci 24:91–105

Winner B, Jappelli R, Maji SK, Desplats PA, Boyer L, Aigner S, Hetzer C, Loher T, Vilar M, Campioni S, Tzitzilonis C, Soragni A, Jessberger S, Mira H, Consiglio A, Pham E, Masliah E, Gage FH, Riek R (2011) In vivo demonstration that alpha-synuclein oligomers are toxic. Proc Natl Acad Sci U S A 108:4194–4199

Wu Z, Asokan A, Samulski RJ (2006) Adeno-associated virus serotypes: vector toolkit for human gene therapy. Mol Ther 14:316–327

Yamada M, Iwatsubo T, Mizuno Y, Mochizuki H (2004) Overexpression of alpha-synuclein in rat substantia nigra results in loss of dopaminergic neurons, phosphorylation of alpha-synuclein and activation of caspase-9: resemblance to pathogenetic changes in Parkinson's disease. J Neurochem 91:451–461

Zarranz JJ, Alegre J, Gomez-Esteban JC, Lezcano E, Ros R, Ampuero I, Vidal L, Hoenicka J, Rodriguez O, Atares B, Llorens V, Gomez Tortosa E, del Ser T, Munoz DG, de Yebenes JG (2004) The new mutation, E46K, of alpha-synuclein causes Parkinson and Lewy body dementia. Ann Neurol 55:164–173

Zigmond MJ, Abercrombie ED, Berger TW, Grace AA, Stricker EM (1990) Compensations after lesions of central dopaminergic neurons: some clinical and basic implications. Trends Neurosci 13: 290–296

Zolotukhin S, Potter M, Zolotukhin I, Sakai Y, Loiler S, Fraites TJ Jr, Chiodo VA, Phillipsberg T, Muzyczka N, Hauswirth WW, Flotte TR, Byrne BJ, Snyder RO (2002) Production and purification of serotype 1, 2, and 5 recombinant adeno-associated viral vectors. Methods 28:158–167